Biochemical Pharmacology 246 (2026) 117725

Contents lists available at ScienceDirect

Biochemical Pharmacology

journal homepage: www.elsevier.com/locate/biochempharm

Neurophysiological and neuropharmacological effects of melatonin MT2 receptors activation in MK-801-induced schizophrenia-like dysfunctions☆

Benedetta Barzon [a], Federica Marchiotto [b], Sofia Nasini [a], Antonino Casile [a,c], Sabina Peluso [b], Carlo Cifani [c], Nikolaos Pitsikas [a], Gabriella Gobbi [d], Marco Cambiaghi [b,f], Stefano Comai [a,d,*]

[a] Department of Pharmaceutical and Pharmacological Sciences, University of Padua, Padua 35131, Italy
[b] Department of Neurosciences, Biomedicine and Movement Sciences, University of Verona, Verona 37124, Italy
[c] School of Pharmacy, Pharmacology Unit, University of Camerino, Via Madonna delle Carceri, 9, Camerino, 62032, Italy
[d] Department of Psychiatry, McGill University, Montreal H3A1A1, QC, Canada
[f] Department of Neurology, Hackensack Meridian School of Medicine, Nutley, NJ 07110, USA

ARTICLE INFO

Keywords:
MT2 receptors
Schizophrenia
MK-801
Parvalbumin positive neurons
Local field potentials
Prefrontal cortex

ABSTRACT

Schizophrenia (SCZ) is a chronic psychiatric disorder characterized by positive, negative, and cognitive symptoms that remain insufficiently controlled by current dopamine- and serotonin-based antipsychotics. Emerging evidence implicates melatonin MT2 receptors in the regulation of the sleep-wake cycle, circadian rhythms and cortical inhibition, both altered in SCZ. Here, we investigated the neuropharmacological effects of the selective MT2 partial agonist UCM924 in the MK-801 model of SCZ-like dysfunctions in male mice. UCM924 (10 mg/kg, intraperitoneally) was selected as a dose not affecting basal locomotion. Acute administration of MK-801 (0.3 mg/kg) induced hyperlocomotion, social interaction abnormalities, and impaired spatial working memory. UCM924 normalized MK-801-induced hyperactivity and social deficits but did not improve cognitive performance. Immunofluorescence analysis revealed that UCM924 increased c-Fos activation in parvalbumin-positive interneurons of the prefrontal cortex, with no effect on tyrosine hydroxylase-positive neurons in the ventral tegmental area. Local field potential recordings showed that UCM924 alone reduced gamma-band power (12–90 Hz) in both regions, whereas MK-801 markedly enhanced it. Co-administration of MK-801 and UCM924 resulted in MK-801-dominant oscillatory patterns, suggesting limited efficacy of MT2 activation in restoring network synchronization. These findings indicate that MT2 receptor stimulation selectively enhances prefrontal inhibitory tone and ameliorates behavioral abnormalities related to positive-like and negative-like symptoms, without normalizing cognitive and electrophysiological deficits. Overall, MT2 receptor-selective drugs may represent promising candidates for targeting specific symptom domains in SCZ through mechanisms distinct from current antipsychotics.

1. Introduction

Schizophrenia (SCZ) is a severe, chronic and heterogeneous psychiatric disorder characterized by profound impairments in social, occupational, and individual functioning, leading to markedly reduced quality of life. The clinical presentation of SCZ encompasses three major symptom domains: (i) positive symptoms, including hallucinations, delusions, thought disorders, hyperactivity, and stereotypies; (ii) negative symptoms, such as social withdrawal, anhedonia, alogia, and avolition; and (iii) cognitive impairments affecting attention, memory, and executive function [1,2]. Currently available antipsychotic drugs provide only partial symptom relief. First-generation antipsychotics or D2 antagonists primarily ameliorate positive symptoms, while second-generation or 5-HT2A antagonist antipsychotics also exert modest

Abbreviations: SCZ, Schizophrenia; MLT, melatonin; i.p., intraperitoneally; OFT, Open Field Test; DMSO, dimethyl sulfoxide; 4-P-PDOT, N-(1,2,3,4-tetrahydro-4-phenyl-2-naphthalenyl)-propanamide; LFP, Local Field Potential; PFC, pre-frontal cortex; VTA, ventral tegmental area; PBS, phosphate-buffered saline; PFA, paraformaldehyde; PV, parvalbumin; TH, tyrosine hydroxylase.

☆ This article is part of a special issue entitled: 'GPCRs in Neuropharmacology' published in Biochemical Pharmacology.

* Corresponding author at: Work Address: Department of Pharmaceutical and Pharmacological Sciences, University of Padua, Largo Meneghetti 2, 35131 Padua, PD, Italy.
E-mail address: stefano.comai@unipd.it (S. Comai).

https://doi.org/10.1016/j.bcp.2026.117725
Received 28 October 2025; Received in revised form 24 December 2025; Accepted 16 January 2026
Available online 20 January 2026

effects on negative symptoms. However, both drug classes are associated with substantial adverse effects, and approximately 30% of patients remains treatment-resistant [3,4]. Consequently, there is an urgent need for novel therapeutic strategies targeting alternative neurobiological mechanisms implicated in SCZ. A very recent example in this direction is the approval by FDA of a new antipsychotic combination consisting of the selective M1/M4 muscarinic receptor agonist xanomeline, which expresses consistent antipsychotic and pro-cognitive properties, and trospium, a peripherally restricted muscarinic antagonist which is able to mitigate peripheral cholinergic side effects (nausea, constipation, and dry mouth) [5,6]. However, the Phase 3 ARISE trial, designed to evaluate this combination as an adjunctive therapy to atypical antipsychotics, did not achieve its primary endpoint indicating that it may have limited effectiveness when used alongside existing antipsychotic treatments [5,6].

Nevertheless, this strategy represents a significant mechanistic shift away from traditional dopamine and/or serotonin receptor antagonism and underscores the ongoing search for therapies with improved efficacy and safety, particularly for addressing negative and cognitive symptoms. Based on the hypothesis that hypofunction of NMDA-type glutamate receptors plays a crucial role in the pathophysiology of SCZ [7,8], non-competitive NMDA receptor antagonists such as MK-801 (dizocilpine) reliably induce SCZ-like behavioral, cognitive, and neurochemical abnormalities in rodents [9,10], making this model a widely used preclinical tool for evaluating candidate antipsychotic compounds.

Increasing attention has been directed toward the role of circadian rhythms dysfunctions in SCZ. Indeed, disruptions in circadian rhythms are a well-documented feature of the disorder and are associated with sleep disturbances, cognitive deficits, and mood dysregulation [11–14]. Dysfunctions in the melatonin (MLT) system may contribute to these abnormalities, being MLT one of the key endogenous regulators of circadian rhythms. Indeed, patients with SCZ display reduced circulating MLT levels and abnormal secretion patterns, including phase advances in plasma MLT rhythms [15–18]. Reduced MLT concentrations have been linked to both cognitive deficits and circadian misalignment [17]. MLT exerts its effects primarily through two G protein-coupled receptors, MT1 and MT2 [15,19]. Over the past decade it has been shown that the MT1 and MT2 receptors subserve distinct functional roles in part due to receptor-specific signaling cascades and regional expression patterns [15,20]. Importantly, pharmacological investigations indicate that selective activation of MT1 or MT2 receptors can yield more targeted therapeutic effects compared to non-selective stimulation by endogenous MLT or non-selective MLT receptors agonists such as ramelteon and tasimelteon [15,20–25]. These findings support the potential advantages of receptor subtype-selective ligands in the development of MLT-based interventions for neuropsychiatric disorders. Andrabi *et al.* [26] showed that MLT exerts neuroprotective effects against MK-801-induced SCZ-like symptoms in mice by improving cognitive and motor performance, reducing oxidative stress, and normalizing neurochemical, molecular, and histopathological alterations in the prefrontal cortex. However, no attempt was made to understand whether these effects were MT1 and/or MT2 receptors mediated. Interestingly, Wang *et al.* [27] showed that MLT reverses MK-801-induced disruptions in sleep timing and intracellular signaling through activation of MT2 and not MT1 receptors. Moreover, in a pilot study conducted in the Iranian population, the variant rs10830963(C/G) of the MT2 receptor gene *MTN1B* was associated with increased risk of developing SCZ [28]. Therefore, in the present study, we have investigated the effects of the selective activation of MT2 receptors by the partial agonist UCM924 [29] in the MK-801 preclinical model of SCZ in which we have evaluated behavioral outcomes relevant to positive, negative (social interaction) and cognitive symptom domains, as well as we have explored potential underlying neurobiological mechanisms. Our aim was to assess the potential of MT2 receptor modulation as a novel target for the therapeutics of SCZ.

2. Material and methods

2.1. Experimental design

Eight-week-old C57BL/6 male mice were randomly assigned to a total of five cohorts. The first cohort (Fig. 1-A) (n = 33) was employed to determine a suitable UCM924 dose that does not affect spontaneous locomotor activity given its sleep-promoting properties [23]. Mice were randomly divided into three experimental groups with n = 11 mice per group as follows: vehicle (0.9% NaCl), UCM924 10 mg/kg and UCM924 20 mg/kg injected intraperitoneally (i.p.). Locomotor activity was assessed using the Open Field Test (OFT). Based on these results of this preliminary study, the 10 mg/kg dose of UCM924 was selected for subsequent experiments.

Three cohorts were each divided into four experimental groups with n = 9–17 mice per group. All animals received two consecutive i.p. injections 10 min apart, and behavioral testing began 10 min after the second injection. This experimental design was designed to assess the therapeutic efficacy of UCM924 against MK-801–induced SCZ-like symptoms. The first group (vehicle + vehicle) received saline followed by 70% dimethyl sulfoxide (DMSO) and 30% saline. The second group (MK-801 + vehicle) received 0.3 mg/kg MK-801 followed by 70% DMSO and 30% saline. The third group (UCM924 + vehicle) received saline followed by 10 mg/kg UCM924, and the fourth group (MK-801 + UCM924) received 0.3 mg/kg MK-801 followed by 10 mg/kg UCM924.

Each cohort was assigned to specific experimental procedures. The second cohort (Fig. 1-B) (n = 42) was tested in the direct sociability test and the T-maze test, with a 10-day interval between the two tests. The third cohort (Fig. 1-C) (n = 50) performed the cage activity test, and the OFT after 10 days. 60 min after the end of the OFT each mouse was perfused, and the brain was collected to perform immunofluorescence reactions. The fourth cohort (Fig. 1-D) (n = 18) underwent local field potential (LFP) recordings.

The fifth cohort (Fig. 1-E) (n = 16) was divided into two experimental groups and performed the OFT and the T-maze test, with a 10-day interval between the two. All animals received two consecutive i.p. injections 10 min apart, and behavioral testing began 10 min after the second injection. The first group (vehicle + MK-801) received 70% DMSO and 30% saline followed by 0.3 mg/kg MK-801. The second group (4-P-PDOT + MK-801) received 10 mg/kg N-(1,2,3,4-tetrahydro-4-phenyl-2-naphthalenyl)-propanamide (4-P-PDOT) followed by 0.3 mg/kg MK-801.

2.2. Drugs

All solutions were freshly prepared on the day of testing and were administered i.p. in a volume of 0.1 ml. N-{2-([3-bromophenyl]-4-fluorophenylamino)ethyl}acetamide (UCM924) (Delmar Chemicals, Inc., Montreal, Canada) was dissolved in 70% DMSO (Merck, Darmstadt, Germany) and 30% saline (0.9% NaCl). Doses of UCM924 were selected based on our previous experiments [22,30]. MK-801 (Cayman Chemical, Ann Arbor, MI, USA) was dissolved in saline. The dose of MK-801 (0–3 mg/Kg) was selected according to Wu *et al.* [31]. 4-P-PDOT (Cayman Chemical, Ann Arbor, MI, USA) was dissolved in 70% DMSO and 30% saline. The dose of 4-P-PDOT was selected based on our previous experiments [32,33].

2.3. Animals

Independent groups of naïve C57BL/6 male mice (2–4 months old, about 23 g body weight) from breeding colonies of the Department of Pharmaceutical and Pharmacological Sciences (University of Padua, Padua, Italy) were used. Animals were housed in Makrolon® cages (45 × 25 × 15 cm), 2 to 5 mice per cage, under standard conditions (21 ± 1 °C; 50–55% relative humidity; 12-h/12-h light/dark cycle, lights on at 7 am and off at 7 pm) with free access to food and water.

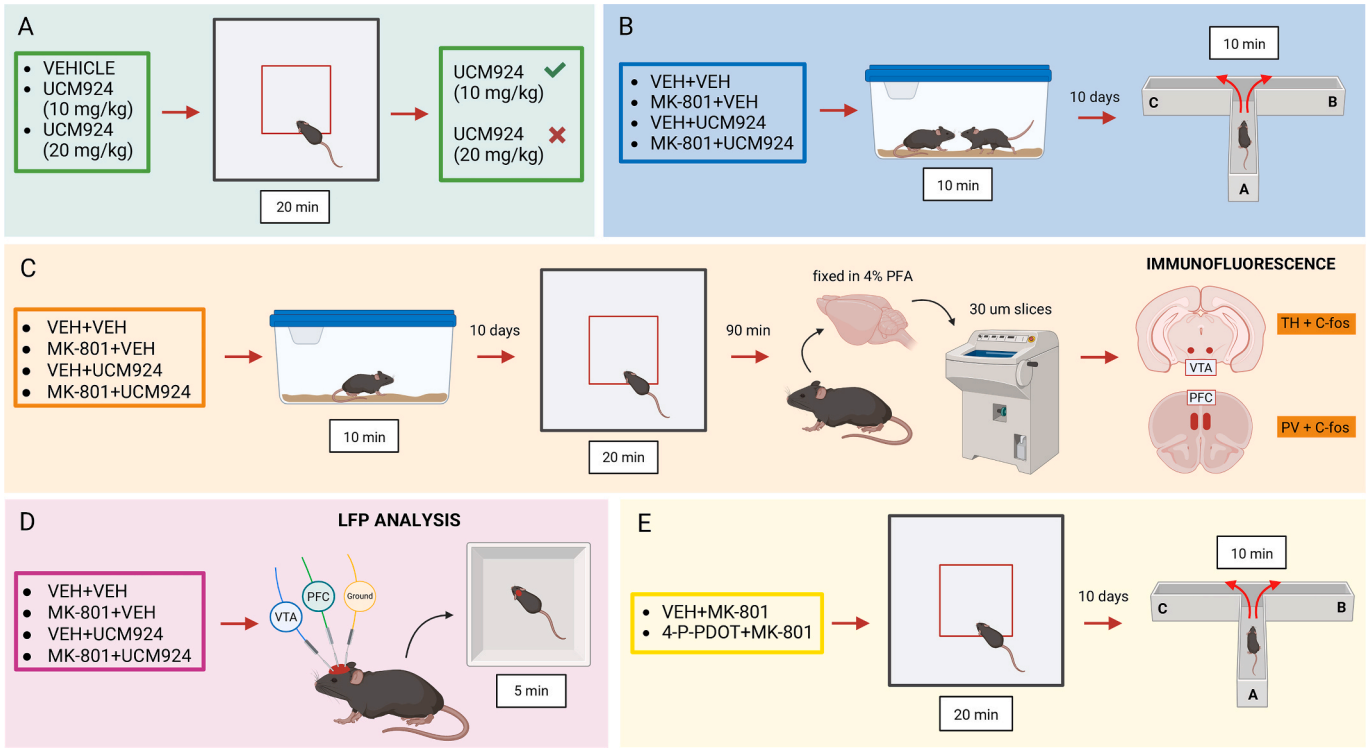

Fig. 1. Experimental design. Schematic representation of the four experimental cohorts (A–E), color-coded, each subjected to distinct procedures. Created in BioRender, https://BioRender.com/sws81u7.

2.4. Behavioral tests

Behavioral testing was performed between 10 am and 3 pm under standard room lighting conditions (350 lx). An interval of at least 10 days was left between tests for recovery. The behavior was recorded using an LCD camera, and activity was automatically tracked using ANY-maze software (Stoelting Europe, Dublin, Ireland). Data were analyzed by experimenters blind to treatment conditions.

2.4.1. Open field test

OFT is a procedure designed to assess spontaneous exploration and locomotor activity in rodents [34]. Mice were individually placed in a square arena (Ugo Basile ®) 40 × 40 cm, with 30 cm high Perspex walls and metal base, and allowed to explore for 20 min. The total distance traveled was measured.

2.4.2. Direct sociability test

The Direct Sociability Test was performed in a home cage with ad libitum access to food and water. The tested animal was placed in the cage and allowed to adapt for 20 min. Afterwards, an unfamiliar sex-, age- and strain-matched conspecific was introduced. The two mice were allowed to freely interact for 10 min, during which social interaction time was manually scored [35].

2.4.3. T-maze test

The T-maze test was performed in a Perspex apparatus (Ugo Basile ®) with a 35 cm long stem and two 30 cm long arms that are 5 cm wide and 15 cm tall according to Deacon *et al.* [36] with slight modifications. Animals were placed in the apparatus and left free to explore for 10mmunofluorescence analysis of PV+/c-Fo-min. Each arm was named with a letter A, B or C. A correct alternation was defined as entries into all three arms consecutively without repetitions (ABC/CBA, BAC/CAB, ACB/BCA). The total number of alternances was defined as the total number of arm entries. The percentage of correct alternances was determined by the ratio of correct alternances to the total, expressed as a percentage.

2.4.4. Home cage activity test

Locomotor activity was recorded in a familiar environment (home cage). After a 20-min adaptation period, activity was recorded for 10-min. Total distance traveled and average speed were quantified.

2.5. Local field potentials (LFP)

To record LFP in the pre-frontal cortex (PFC) and ventral tegmental area (VTA) at the different experimental conditions, mice were first implanted with deep electrodes. Mice were anesthetized by an i.p. injection of ketamine-xylazine (80 mg/kg and 5 mg/kg, respectively) and placed on a stereotaxic frame. Electrodes of tungsten wires (Ø 75 µm, cod. 791100, AM Systems, Washington, USA) were implanted in the right PFC (AP = +1.5 mm, ML = 0.4 mm from Bregma and DV = −2.5 mm from the brain surface) and right VTA (AP = −3.2 mm, ML = 0.5 mm from Bregma and DV = −4.3 mm from the brain surface), with the reference electrode over the left parietal cortex. Extracellular field potentials were recorded in awake, freely moving mice, starting 10 min after the last injection. At the end of the recording session, mice were sacrificed to verify the location of the electrodes by Cresyl Violet (Merck, Darmstadt, Germany) staining. A customized Python script was used for offline power spectrum analysis, for which three epochs of 2 s were averaged. LFP epochs were visually examined for artifacts, and 2-second segments were computed using fast Fourier transforms by using a customized Python Script for power spectral analysis. Mean power spectra (4–5 mice/group) of PFC and VTA were compared among groups and divided into frequency bands for statistical analysis. Relative power was calculated by dividing the absolute amplitude within the specified frequency ranges by the total amplitude. The following frequency bands were used: delta (0.5–4 Hz), theta (4–12 Hz), beta (12–20 Hz), low-gamma (20–50 Hz), and high-gamma (50–90 Hz).

2.6. Perfusion and tissue collection

Mice were perfused transcardially with 0.9% saline followed by 4% paraformaldehyde (PFA, Merck, Darmstadt, Germany) in phosphate-buffered saline (PBS, Merck, Darmstadt, Germany). Brains were post-fixed in 4% PFA for 3 h, cryoprotected in 30% sucrose in PBS, frozen, and stored at −20 °C.

2.7. Immunohistochemistry

c-Fos activation in parvalbumin-positive (PV+) interneurons was analyzed in the prefrontal cortex (PFC; Bregma + 1.70 mm). Free-floating coronal brain sections (30 μm thick) were washed in PBS and subjected to antigen retrieval by incubation in citrate buffer at 95 °C. Sections were blocked for 1 h at room temperature in a solution containing 4% normal donkey serum and 0.3% Triton X-100 in PBS. Primary antibodies (rabbit anti-c-Fos, 1:1000, Synaptic Systems, Göttingen, Germany; mouse anti-PV, 1:1000, Abcam, Cambridge, UK) were applied, and sections were incubated for two overnights at 4 °C. After PBS washes, Alexa Fluor-conjugated secondary antibodies were applied (donkey anti-rabbit Cy5, 1:400, Abcam, Cambrige, UK; donkey anti-mouse AF555, 1:400, Jackson ImmunoResearch, West Grove, PA, USA) for 2 h at room temperature. Nuclei were counterstained with DAPI (1:5000, Invitrogen, Massachusetts, USA), and sections were mounted using antifade mounting medium (Dako; Merck, Darmstadt, Germany).

c-Fos activation in tyrosine hydroxylase-expressing (TH+) neurons was analyzed in the ventral tegmental area (VTA; Bregma − 3.16 mm). Sections were processed similarly to those described above for PV+ staining. After PBS washes and antigen retrieval (citrate buffer, 95 °C), sections were blocked for 1 h in 3% normal goat serum, 0.5% bovine serum albumin, and 1% Triton X-100 in PBS. Primary antibodies (rabbit anti-c-Fos, 1:1000, Synaptic Systems, Göttingen, Germany; mouse anti-TH, 1:1000, GeneTex, San Antonio, TX, USA) were applied and incubated for two overnights at 4 °C. After PBS washes, appropriate secondary antibodies (goat anti-rabbit CF594, 1:400, Sigma-Aldrich, Darmstadt, Germany; goat anti-mouse AF488, 1:400, Jackson ImmunoResearch, West Grove, PA, USA) were applied for 2 h at room temperature. Nuclei were counterstained with DAPI (1:5000, Invitrogen, Massachusetts, USA), and sections were mounted with antifade medium (Dako; Merck, Darmstadt, Germany).

Images were acquired using a confocal laser scanning microscope (Zeiss LSM800).

2.8. Images analysis

Images (z-stack projections) were analyzed using QuPath v0.5.1. For each experimental condition, 2 sections per animal were analyzed. Marker-positive neurons (PV+ or TH+) were identified using the cell detection tool in QuPath. For each detected PV+ or TH+ cell, the mean fluorescence intensity in the c-Fos channel was extracted. To assess c-Fos activation, z-scores were calculated from the c-Fos intensity distribution within each image. PV+ cells were classified as c-Fos positive if their z-score was greater than 0, and negative otherwise. TH+ cells were considered c-Fos positive when their z-score exceeded 1, and negative when below this threshold. All quantifications were performed blind to experimental conditions.

2.9. Statistical analysis

Data were expressed as mean ± standard error of the mean (SEM). Statistical analyses were performed using GraphPad Prism 8.2.1. Data distribution was analyzed using the Shapiro-Wilk test. When data were normally distributed, Student's *t*-test or one-way or two-way analysis of variance (ANOVA) test followed by Bonferroni's multiple comparisons test was used. When data were non-normally distributed, Mann-Whitney test or Kruskal-Wallis test followed by Dunn's multiple correction was used. A P value of <0.05 was considered significant.

3. Results

3.1. UCM924 dose-finding study

We first performed a dose–response curve with UCM924 to find a dose of UCM924 that does not affect spontaneous locomotor activity given the known hypnotic/sedative properties of MT2 partial agonists [37] that may confound the effects of the drug on SCZ-like symptoms such as hyperactivity. Therefore, the 10 and 20 mg/kg doses of UCM924 were assessed in the OFT. The distance traveled during the 20-min session was significantly affected by UCM924 treatment (Fig. 2; one-way ANOVA, $F(2,30) = 10.61$, $P = 0.0003$). UCM924 at a dose of 10 mg/kg did not alter the total distance traveled relative to vehicle controls whereas UCM924 at a dose of 20 mg/kg significantly reduced the total distance traveled compared to both vehicle ($P = 0.0002$) and UCM924 10 mg/Kg ($P = 0.0301$) treated animals. Based on these findings, 10 mg/kg was selected for subsequent experiments.

3.2. Open field test

This task was used to assess the effects of UCM924 on MK-801-induced hyperlocomotion, a well-validated correlate of positive-like symptoms in rodent models of SCZ. In the OFT, the total distance traveled was significantly influenced by MK-801 pre-treatment and UCM924 treatment (Fig. 3-B; two-way ANOVA; UCM924 treatment: $F(1,46) = 6.236$, $P = 0.0159$; MK-801 pre-treatment: $F(1,46) = 21.68$, $P < 0.0001$, interaction: $F(1,46) = 4.115$, $P = 0.0483$). Animals treated with MK-801 traveled a longer distance compared to the control group (MK-801 + vehicle vs vehicle + vehicle: $P = 0.0002$). UCM924 significantly attenuated this hyperlocomotion (MK-801 + UCM924 vs MK-801 + vehicle: $P = 0.0148$), reducing the activity in MK-801-treated mice to control levels (MK-801 + UCM924 vs vehicle + vehicle: $P = 0.8075$).

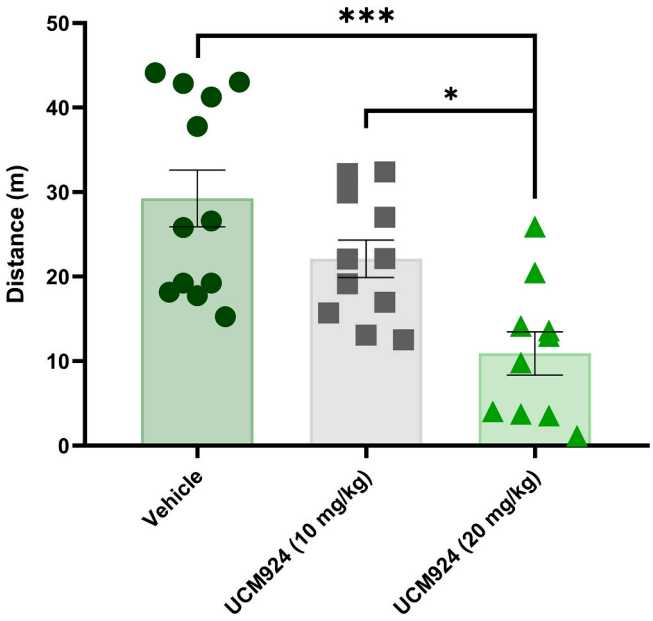

Fig. 2. Dose related effect of UCM924 on locomotor activity. Total distance traveled during the 20-min OFT. Data are presented as mean ± SEM (n = 11–12 mice per group). * $p < 0.05$, *** $p < 0.001$; one-way ANOVA followed by Bonferroni post-hoc comparisons.

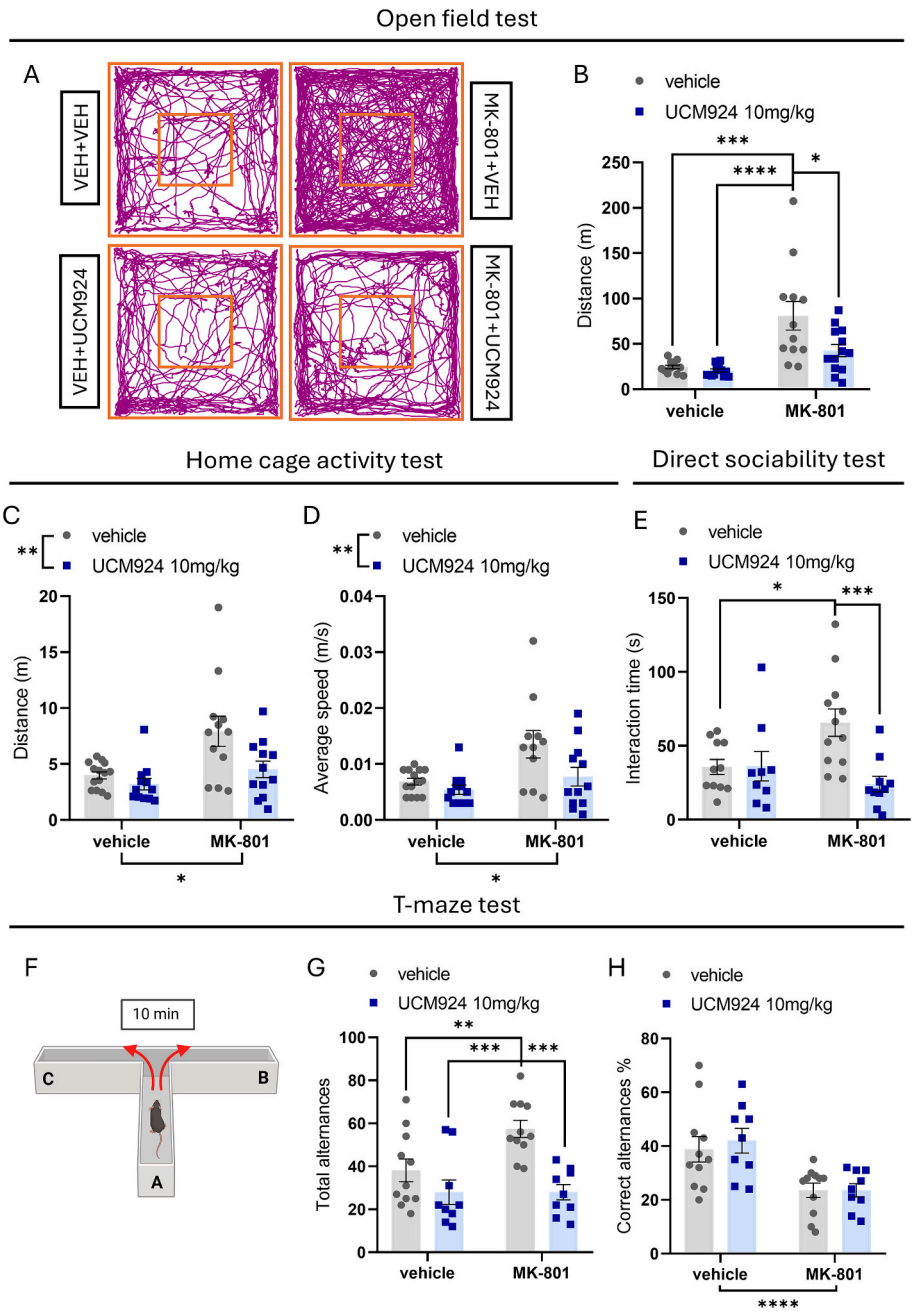

Fig. 3. Behavioral assessment of MK-801-induced deficits and their reversal by UCM924. (A) Representative track plot for each experimental group of the path followed during the OFT. (B) Total distance traveled during the OFT. (C) Total distance traveled, and (D) average speed during the 10 min home cage activity evaluation. (E) Time of interaction during the direct sociability test. (F) Schematic representation of the T-maze test. (G) Number of total alternances, and (H) percentage of correct alternances made during the T-maze test. Data are presented as mean ± SEM (n = 10–14 mice per group). * $p < 0.05$, ** $p < 0.01$, *** $p < 0.001$, **** $p < 0.0001$; two-way ANOVA followed by Bonferroni post-hoc comparisons. Part of this figure was created in BioRender, https://BioRender.com/t69bxqy.

3.3. Home cage activity test

We tested the effects of UCM924 on MK-801-induced effect on locomotor activity also in the home cage, a minimally stressful environment, to validate whether changes in locomotion reflect true behavioral modulation rather than novelty-induced responses. Both the distance traveled (Fig. 3-C; two-way ANOVA; UCM924 treatment: $F(1,46) = 10.38$, $P = 0.0019$; MK-801 pre-treatment: $F(1,46) = 6.849$, $P = 0.0120$, interaction: $F(1,46) = 2.686$, $P = 0.1080$) and the average speed (Fig. 3-D; two-way ANOVA; UCM924 treatment: $F(1,45) = 9.405$, $P = 0.0037$; MK-801 pre-treatment: $F(1,45) = 6.051$, $P = 0.0178$, interaction: $F(1,46) = 2.192$, $P = 0.1457$) during the 10-min test were significantly influenced by pre-treatment with MK-801 and UCM924 treatment, with no interaction pre-treatment × treatment. Animals treated with MK-801 showed increased locomotor activity, traveling a longer distance and moving at a higher average speed compared to vehicles, regardless of UCM924 treatment. Treatment with UCM924 reduced both the total distance traveled and the average speed, regardless of MK-801 pre-treatment.

3.4. Direct sociability test

We underwent the direct sociability test to probe social interaction deficits that are hallmark features of SCZ. In this task, a significant effect of MK-801 pre-treatment and UCM924 treatment and an interaction between the two factors were observed (Fig. 3-E; two-way ANOVA; UCM924 treatment: $F(1,38) = 1.338$, $P = 0.2546$; MK-801 pre-treatment: $F(1,38) = 7.008$, $P = 0.0117$, interaction: $F(1,38) = 7.319$, $P = 0.0102$). MK-801 treated animals spent significantly more time interacting with the unfamiliar conspecific compared to vehicle animals (MK-801 + vehicle vs vehicle + vehicle: $P = 0.0398$). Treatment with UCM924 reduced the interaction time in MK-801 treated animals (MK-801 + vehicle vs MK-801 + UCM924: $P = 0.0024$), bringing it back to control levels (MK-801 + UCM924 vs vehicle + vehicle: $P > 0.9999$). In animals treated with UCM924 alone, no increase in interaction time was observed compared to control animals (vehicle + UCM924 vs vehicle + vehicle: $P > 0.9999$).

3.5. T-maze test

The T-maze spontaneous alternation task assesses spatial working memory, a cognitive domain frequently impaired in SCZ and sensitive to NMDA receptor dysfunction. In this test, a significant effect of pre-treatment and treatment and an interaction between the two factors was observed on the total number of alternances (Fig. 3-G; two-way ANOVA; UCM924 treatment: $F(1,36) = 4.115$, $P = 0.0499$; MK-801 pre-treatment: $F(1,36) = 17.41$, $P = 0.0002$, interaction: $F(1,36) = 4.115$, $P = 0.0499$). MK-801 treated animals performed a significantly higher number of correct alternances compared to control animals (MK-801 + vehicle vs vehicle + vehicle: $P = 0.0275$). Treatment with UCM924 in MK-801-treated animals reduced the number of alternances back to control levels (MK-801 + vehicle vs MK-801 + UCM924: $P = 0.0006$). In animals treated with UCM924 alone, the number of alternances did not differ significantly from the control group and was significantly lower compared to MK-801-treated animals (MK-801 + vehicle vs vehicle + UCM924: $P = 0.0006$).

A significant effect of pre-treatment but not of treatment and no interaction were found on the percentage of correct alternances (Fig. 3-H; two-way ANOVA; UCM924 treatment: $F(1,36) = 0.1754$, $P = 0.6778$; MK-801 pre-treatment: $F(1,36) = 19.58$, $P < 0.0001$, interaction: $F(1,36) = 0.1732$, $P = 0.6797$). MK-801-treated animals showed a significant reduction in the percentage of correct alternances compared to control animals, regardless of the UCM924 treatment.

3.6. MT2 receptor blockade does not modify MK-801–induced behavioral alterations

To determine whether endogenous MT2 receptor signaling contributes to the expression of MK-801–induced SCZ-like behaviors, we pharmacologically blocked MT2 receptors using the selective antagonist 4-P-PDOT [38] prior to behavioral testing. Pre-treatment with 4-P-PDOT did not modify MK-801–induced hyperlocomotion in the Open Field Test, as no differences were observed in the total distance traveled between MK-801–treated mice receiving 4-P-PDOT and those receiving vehicle (Fig. 4-B; Student's *t*-test: $t = 0.1986$, $df = 14$, $P = 0.8454$). Similarly, MT2 receptor blockade did not affect MK-801–induced alterations in spatial working memory in the T-maze task. No differences were detected between treatment groups in either the total number of alternations (Fig. 4-C; Mann–Whitney test: $U = 22.50$, $P = 0.3420$) or the percentage of correct alternations (Fig. 4-D; Mann–Whitney test: $U = 22.50$, $P = 0.3346$). To note, administration of 10 mg/kg 4-P-PDOT alone did not affect locomotor activity or T-maze performance compared with vehicle-treated controls (data not shown).

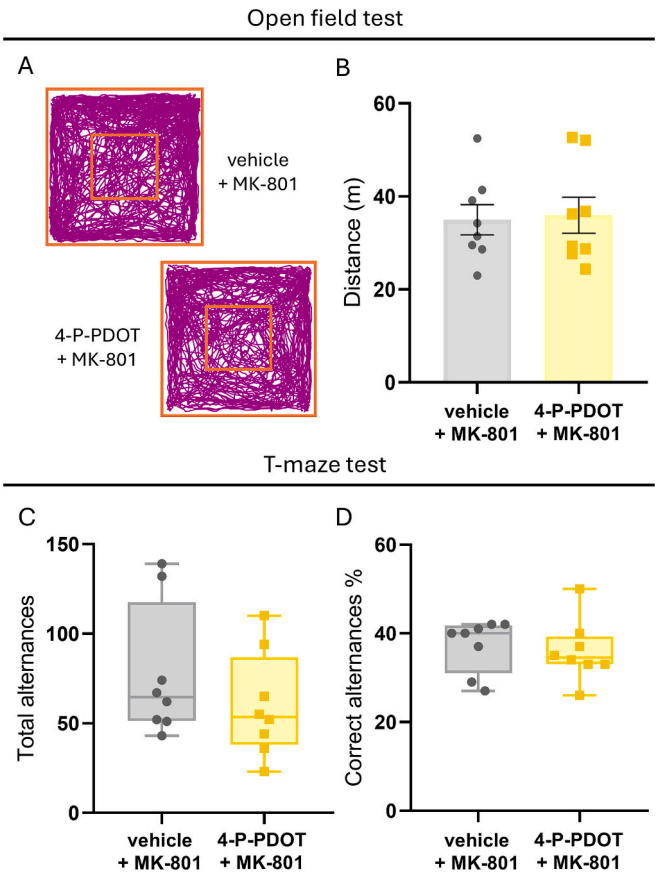

Fig. 4. Effect of the MT2 receptor blockade with 4-P-PDOT on MK-801 induced SCZ-like symptoms (A) Representative track plot for each experimental group of the path followed during the OFT. (B) Total distance traveled during the OFT. (C) Number of total alternances, and (D) percentage of correct alternances made during the T-maze test. Data are presented as mean ± SEM (B) and median with min to max (C, D) (n = 8 mice per group).

3.7. Immunohistochemistry

Immunohistochemical analysis and also electrophysiological measures were conducted in the PFC and VTA because they are key nodes in the mesocorticolimbic circuitry, whose dysregulation represents a central pathophysiological feature of SCZ [39]. Treatment with UCM924 increases the percentage of PV+/c-Fos+ interneurons in the PFC regardless of the pre-treatment with MK-801 (Fig. 5-D; two-way ANOVA; UCM924 treatment: $F(1,17) = 11.53$, $P = 0.0034$; MK-801 pre-treatment: $F(1,17) = 0.5643$, $P = 0.4628$, interaction: $F(1,17) = 2.505$, $P = 0.1319$). No difference between treatment groups was seen in the percentage of TH+/c-Fos+ neurons in the VTA (Fig. 5-F; two-way ANOVA; UCM924 treatment: $F(1,17) = 1.395$, $P = 0.2538$; MK-801 pre-treatment: $F(1,17) = 5.243$, $P = 0.0351$, interaction: $F(1,17) = 1.377$, $P = 0.2568$).

3.8. Local field potentials

Power spectral analysis of the PFC revealed that, compared with the control group (vehicle + vehicle), mice treated with MK-801 (MK-801 + vehicle) exhibited a significant increase in gamma band power (Fig. 6-F; mean rank difference = −87.23 and −62.93; Kruskal-Wallis test, Dunn's multiple correction <0.001, respectively). A similar effect was observed in the VTA, where high-gamma power was enhanced (Fig. 6-H; mean rank difference = −64.58; Kruskal-Wallis test, Dunn's multiple correction <0.001). In contrast, mice receiving UCM924 alone (vehicle + UCM924) showed a marked reduction in power across the entire 12–90

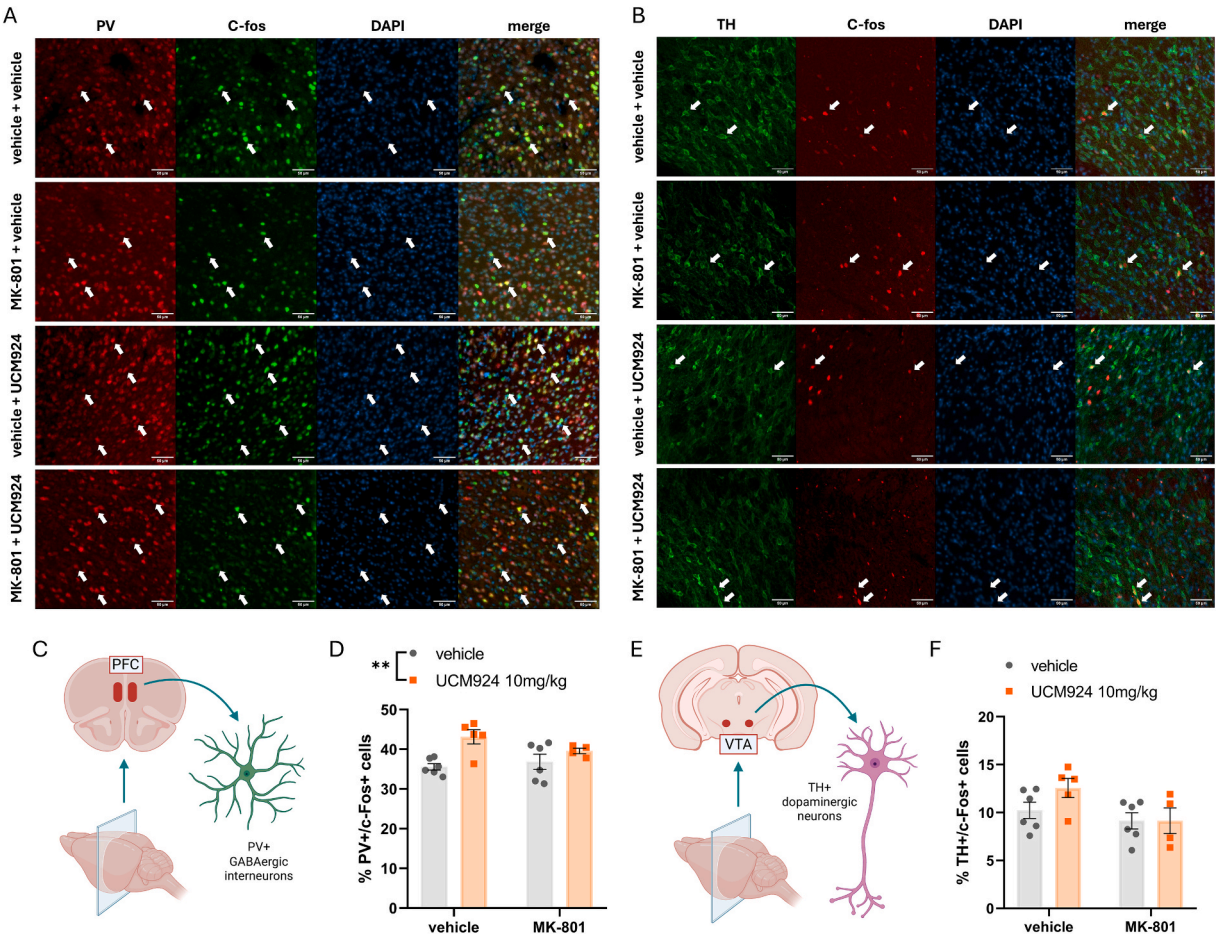

Fig. 5. Immunofluorescence analysis of PV+/c-Fos+ neurons in the PFC and TH+/c-Fos+ neurons in the VTA. (A) Representative confocal images showing PV+ neurons (red), c-Fos+ nuclei (green), and colocalization (yellow) in merged channels. Nuclei were counterstained with DAPI (blue). (B) Representative confocal images showing TH+ neurons (green), c-Fos+ nuclei (red), and colocalization (yellow) in merged channels. Nuclei were counterstained with DAPI (blue). (C) Schematic representation of PFC and GABAergic interneurons. (D) Percentage of PV+/c-Fos+ cells in the PFC. (E) Schematic representation of VTA and dopaminergic neurons. (F) Percentage of TH+/c-Fos+ cells in the VTA. Data are presented as mean ± SEM (n = 4–6 mice per group). ** $p < 0.01$; two-way ANOVA followed by Bonferroni post-hoc comparisons. Part of this figure was created in BioRender, https://BioRender.com/ouuj45l.

Hz range in both regions (Fig. 6-F,H; PFC: mean rank difference = 25.0, 62.42 and 114.9; VTA: mean rank difference = 30.69, 77.2 and 102; Kruskal-Wallis test, Dunn's multiple correction < 0.001). When MK-801 and UCM924 were co-administered (MK-801 + UCM924), spectral power increased across the full gamma range in both the PFC (Fig. 6-F; mean rank difference = −80.25 and −49.02) and VTA (Fig. 6-H; mean rank difference = −92.5 and −94.96; Kruskal-Wallis test, Dunn's multiple correction < 0.01), indicating a dominant effect of MK-801. By contrast, low-frequency bands (delta, 0.5–4 Hz; theta, 4–12 Hz) were not significantly affected under any treatment condition in either brain region (Fig. 6-E,G; Kruskal-Wallis test, P > 0.05).

4. Discussion

In this study we investigated the neuropharmacological effects of selective MT2 receptor activation by the partial agonist UCM924 in the MK-801 model of SCZ-like dysfunctions. We found that UCM924 normalized MK-801-induced hyperactivity and social deficits but failed to ameliorate cognitive impairments in spatial memory. These behavioral effects occurred at a dose not affecting basal locomotor activity but also known not to induce sleep [23]. At the cellular level, UCM924 increased the activation of PV+ interneurons in the PFC but had no effect on TH+ dopaminergic neurons in the VTA. This selective activation pattern is particularly relevant for understanding the circuit-level effects of UCM924. The lack of PV+ activation in the VTA, contrasted with the marked increase in the PFC, indicates that MT2 receptor–mediated modulation primarily occurs within cortical inhibitory networks rather than at the level of midbrain dopaminergic neurons. This regional specificity is consistent with MT2 receptor distribution reported by Lacoste *et al.* [40], who demonstrated receptor expression in GABAergic PV+ regions such as the reticular thalamic nucleus but not in the VTA. In parallel with behavioral and immunohistochemical data, LFP recordings in the VTA and PFC, revealed that MK-801 produced robust increases in gamma-band activity in both the PFC and VTA, consistent with aberrant network synchronization typically associated with NMDAR hypofunction. In contrast, UCM924 reduced the power across the 12–90 Hz range in both regions. Of interest, when MK-801 and UCM924 were co-administered, the effect of MK-801 was predominant. Taken together, these findings indicate that MT2 receptor activation selectively engages PFC interneurons and modulates cortical and mesolimbic oscillatory activity, but its capacity to counteract NMDAR antagonist–induced network dysfunction is limited to certain behavioral domains. Finally, we found that blockade of MT2 receptors with the selective MT2 antagonist 4-P-PDOT did not influence MK-801–evoked SCZ-like behaviors, suggesting that MK-801 does not exert its effects through MT2 receptor signaling. Moreover, the absence of any effect of 4-P-PDOT administered alone indicates a lack of tonic melatonergic (MT2-mediated) signaling at the time of testing. The administration of MK-801 resulted in increased neural oscillation power in the gamma frequencies especially in the PFC, further confirming the results by Cui *et al.*

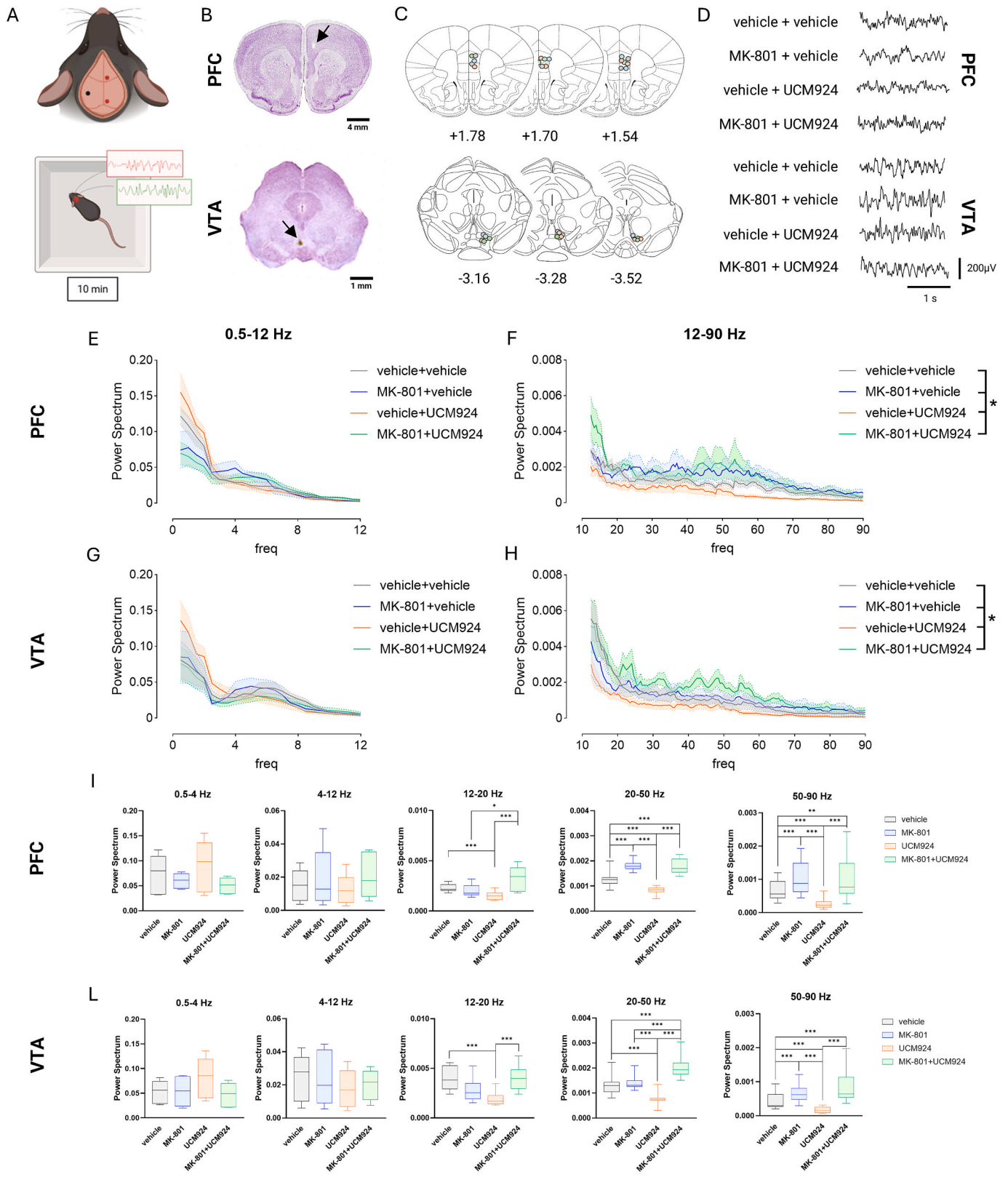

Fig. 6. Local field potential analysis of MK-801- and UCM924- induced changes in PFC-VTA power spectrum. (A) Schematic of the PFC and VTA electrodes (red) and of the contralateral parietal reference electrode (black) location, with the LFP recording setting, below. (B) Representative histology of electrode tracks by Nissl staining in the PFC (top, scale bar = 4 mm) and in the VTA (bottom, scale bar = 1 mm), with the black arrow indicating the electrode site. (C) Location of electrode tips for LFPs recordings in PFC (above) and VTA (below). (D) Example of LFP traces recorded in PFC (above) and VTA (below). PFC (E, F) and VTA (G, H) power spectra from 0.5 to 12 Hz and from 12 to 90 Hz, respectively. Box and Whisker plot of the power spectra in PFC (I) and VTA (L) at different frequency bands: delta (0.5–4 Hz), theta (4–12 Hz), beta (12–20 Hz), low-gamma (20–50 Hz), and high-gamma (50–90 Hz). Data are presented as mean ± SEM (E, F, G, H) and median with min to max (I, L) (n = 4–5 mice per group). * $p < 0.05$, ** $p < 0.01$, *** $p < 0.001$; Kruskal–Wallis test followed by Dunn's multiple correction. Part of this figure was created in BioRender, https://BioRender.com/53vwkmz.

[41] at the same dosage (0.3 mg/kg). In rodents, pharmacological modulation of NMDA receptors has been directly implicated in the regulation of gamma-band oscillations, a key neural rhythm associated with sensory processing and cognitive function. Administration of NMDA receptor antagonists, such as MK-801 or ketamine, leads to aberrant increases in gamma power and desynchronization, which parallel the behavioral disturbances observed in these models [42], including hyperlocomotion and cognitive deficits [43,44]. Importantly, these alterations in neural oscillations are considered to reflect disrupted excitation-inhibition balance within cortical microcircuits [45], particularly involving PV+ GABAergic interneurons that are critically dependent on NMDA receptor signaling for proper function [46].

Similar abnormalities in gamma-band activity have been consistently reported in patients with SCZ, both at rest and during engagement in cognitive tasks such as working memory or attention paradigms [47]. This translational convergence supports the view that disrupted gamma oscillations represent a mechanistic link between NMDAR hypofunction and cortical network desynchronization underlying SCZ symptomatology. While UCM924 alone reduced gamma power, it did not prevent MK-801-induced abnormalities in either PFC or VTA, suggesting that MT2 receptor-mediated effects are circuit- and function-specific. The decrease of gamma-band observed with UCM924 alone, supports the notion that MT2 agonism has mostly hypnotic and analgesic effects with increased delta-band activity (characteristic of deep sleep and analgesia) [30,48], more than pro-cognitive effects or effects on attention and working memory (underlined by gamma activity). Moreover, the fact that UCM924 normalized hyperactivity and social behavior along with the fact that selectively increase activation of PV+ in the PFC, implies that MT2-driven activation of PFC interneurons may suffice to restore local inhibitory tone and ameliorate positive-like symptoms, whereas the re-establishment of large-scale oscillatory coherence is likely required for cognitive processes. This interpretation aligns with the notion that distinct SCZ symptom domains depend on partially overlapping neural substrate [49–51]. Notably, in previous work, we demonstrated that MK-801 disrupts sleep regulation by prolonging circadian period length and delaying non-rapid eye movement (NREM) sleep onset, effects fully reversed by MLT through MT2 receptors [27].

MLT dysregulation has long been associated with SCZ, with evidence of reduced nocturnal secretion and circadian misalignment that may contribute to sleep and cognitive disturbances [18,52–55]. Beyond its role in circadian and sleep regulation, MLT also exerts antioxidant and neuroprotective actions that may counteract oxidative stress and dopaminergic dysregulation, two mechanisms strongly implicated in the pathophysiology of SCZ [56–61]. However, the limited therapeutic efficacy of MLT likely reflects its short half-life and the differential distribution and sometimes opposing effects mediated by MT1 and MT2 receptors. From a drug development perspective, receptor selectivity appears crucial. While non-selective melatonergic ligands (e.g., ramelteon, tasimelteon) activate both MT1 and MT2 receptors, selective approaches may allow for more precise therapeutic outcomes [15,20,22]. MT2 receptors, in particular, have been linked to the regulation of anxiety, nociception, and NREM sleep [30,48,62], while MT1 receptors more strongly influence mood regulation, REM sleep, and neurodegenerative processes [21,24,25,63,64]. In keeping, the fact that not all MK-801-induced symptom domains were rescued by MT2 receptor activation could suggest that MT1 receptors may also play a complementary or distinct role, particularly in cognitive regulation, and this aspect remains to be clarified. Another interesting finding of our study is that 4-P-PDOT was not affecting the response to MK-801 administration, confirming that the mechanism of MK-801 is independent from MT2 receptors. Moreover, 4-P-PDOT alone has no effects on the observed behavior suggesting that it is a pure neutral antagonist and that there is an absence of tonic MLT MT2 receptor activity and low endogenous level of MLT under typical daytime testing conditions. This observation recapitulates data observed in MT2 receptors knockout animals, in which, during the day, we did not observe significant changes in locomotor behavior [62]. In contrast, selective pharmacological activation of MT2 receptors with the exogenous agonist UCM924 produces a high amplitude, supraphysiological engagement of MT2 signaling, independent of endogenous MLT levels. MT2 receptors are Gi/o-coupled [19] and, when activated, can reduce presynaptic glutamate release and stabilize excitatory/inhibitory balance. Consistent with this mechanism, we have observed activation of PV+ interneurons, a cell population critically involved in regulating cortical network synchrony. These processes are directly relevant to the circuits affected by MK-801, which induces SCZ-like alterations by producing excessive cortical and subcortical excitatory drive via NMDA-receptor blockade. To date, there is essentially no robust evidence in humans supporting a role for MT2 receptors in the pathophysiology of SCZ. The only preliminary indication comes from a pilot study in an Iranian cohort reporting that the MTNR1B gene variant rs10830963 (C/G) may be associated with increased SCZ risk [28]. Given also the lack of effects of 4-P-PDOT on MK-801-induced symptoms, we can hypothesize that MT2 receptors are not probably involved in the pathophysiology of SCZ, but when pharmacologically activated, they can exert a “compensatory” or “protective” influence on the abnormal circuitry engaged by NMDA receptor blockade at the bases of SCZ-like symptoms.

Some limitations of the present work should be acknowledged. First, we examined only acute administration and thus whether chronic MT2 receptors activation produces sustained efficacy or tolerance remains unknown. Second, while we observed enhanced PV+ interneuron activation, the intracellular signaling cascades linking MT2 receptor activation to interneuron recruitment remain to be elucidated, for example through scRNA-seq or pathway-specific pharmacological tools. Third, all our experiments were exclusively conducted in male mice. Although the prevalence of SCZ is comparable between sexes, clinical expression differs markedly between males and females. For instance, men more frequently show an earlier age of onset [65,66]. Men also more often exhibit prominent negative symptoms and cognitive deficits, while women tend to have better premorbid social functioning, a later onset (often in the late twenties or with a second incidence peak after age 40), and a generally more favorable course [66–68]. Beyond clinical phenotype, circadian and MLT-related physiology also shows sex differences which could be relevant for melatonergic modulation. In humans, women exhibit a shorter intrinsic circadian period and show earlier timing of core-body temperature nadirs, as well as higher nocturnal MLT amplitude and an advanced phase of MLT secretion, compared with men [69–71]. Across species, evidence indicates that MLT signaling is sexually dimorphic, affecting both behavior, circadian regulation and response to exogenous MLT. For example, in rats, chronic MLT administration produces sex-dependent behavioral effects, with males and females responding differently in paradigms such as the forced swim and open-field tests [72]. In humans, physiological MLT rhythms also differ between sexes, with distinct phase-angle relationships and nocturnal MLT amplitudes, suggesting intrinsic sex differences in MLT production and circadian regulation [70]. Complementing these findings, work in avian models shows that MLT receptor activity in the forebrain is influenced by both sex and environmental context, demonstrating that MLT receptor signaling itself can be sexually differentiated [73]. However, the effects of sex on the melatonergic system and the response to melatonergic drugs remain poorly explored. Nevertheless, given the available evidence, it is likely that sex-dependent differences in both SCZ and MLT/circadian biology could influence the therapeutic response to MT2 receptor activation. Future studies including female animals are therefore warranted to determine whether our findings generalize across sexes or reveal sex-specific dynamics.

Overall, the present findings suggest that MT2 receptor activation may represent a novel therapeutic avenue in SCZ, distinct from conventional dopamine- or glutamate-targeting strategies. Our results support the hypothesis that MT2 selective agonists can engage PFC inhibitory circuits and modulate cortical oscillatory dynamics, offering a

mechanistic rationale for further exploration of MT2-selective drugs as potential therapeutic candidates. By restoring excitation–inhibition balance at the circuit level, MT2-targeted interventions may influence social and negative symptoms, which often remain refractory to current antipsychotics. The impact on cognitive dysfunction, however, remains uncertain and warrants additional investigation. In addition to circuit-level effects, MT2 receptors regulate circadian and sleep processes [15], which are consistently disrupted in SCZ and closely linked to symptom severity, cognitive deficits, and functional outcomes [74,75]. This dual action suggests that MT2 agonists could provide multimodal benefits, simultaneously supporting network dynamics and sleep/wake architecture, an advantage not typically offered by conventional therapies. For example, recently approved compounds such as xanomeline/trospium chloride have shown negative effects on sleep architecture in preclinical models, including reduced NREM sleep quality and quantity [76], highlighting the need for strategies that preserve or enhance sleep integrity. Although additional work is required, MT2 agonists may also have potential as adjunctive therapies, complementing existing antipsychotic regimens by targeting complementary mechanisms, improving sleep quality, and potentially enhancing efficacy without worsening side-effect profiles. Taken together, these results provide a rationale for further preclinical and clinical evaluation of MT2-selective agonists, both as stand-alone and combination therapies. Future studies should carefully investigate optimal dosing and circadian timing, as well as possible synergistic interactions with standard treatments to fully assess the multimodal therapeutic potential of MT2-targeted interventions in SCZ.

CRediT authorship contribution statement

Benedetta Barzon: Writing – original draft, Methodology, Investigation, Data curation, Conceptualization. **Federica Marchiotto:** Writing – original draft, Methodology, Investigation, Data curation. **Sofia Nasini:** Methodology, Investigation, Data curation. **Antonino Casile:** Methodology, Investigation, Data curation. **Sabina Peluso:** Investigation, Data curation. **Carlo Cifani:** Writing – review & editing, Investigation. **Nikolaos Pitsikas:** Writing – original draft, Investigation. **Gabriella Gobbi:** Writing – original draft, Investigation. **Marco Cambiaghi:** Writing – original draft, Supervision, Methodology, Investigation. **Stefano Comai:** Writing – review & editing, Writing – original draft, Validation, Supervision, Methodology, Investigation, Funding acquisition, Data curation, Conceptualization.

Declaration of competing interest

The authors declare the following financial interests/personal relationships which may be considered as potential competing interests: GG is an inventor of patents in MT2 selective drugs. The other authors have no competing financial interests or personal relationships that could have appeared to influence the work reported in this paper.

Acknowledgments

The authors acknowledge Ms. Angelica Maria Zuliani, Sofia Xausa, Valeria Benvenuti and Luana Rasera for technical support.

Fundings

This work was supported by a PRID-J grant from the Department of Pharmaceutical and Pharmacological Sciences, University of Padua, Italy to SC and GG holds the Canadian Research Chair in Therapeutics for Mental Health.

Ethics approval

All experimental procedures were performed in accordance with institutional and ethical guidelines for animal research to ensure animal welfare and minimize distress. The experimental protocol was reviewed and approved by the Institutional Animal Care and Use Committee of the University of Padova and was authorized by the Italian Ministry of Health (authorization n. 41451.32).

Data availability

Data are available upon reasonable request to the corresponding author.

References

[1] T.R. Insel, Rethinking schizophrenia, Nature 468 (7321) (2010) 187–193.
[2] M.F. Green, Cognitive impairment and functional outcome in schizophrenia and bipolar disorder, J. Clin. Psychiatry 67 (Suppl 9) (2006) 3–8, discussion 36–42.
[3] S. Miyamoto, et al., Pharmacological treatment of schizophrenia: a critical review of the pharmacology and clinical effects of current and future therapeutic agents, Mol. Psychiatry 17 (12) (2012) 1206–1227.
[4] J.M. Rubio, J.M. Kane, The pharmacological treatment of schizophrenia: how far have we come? PCN Rep 1 (2) (2022) e13.
[5] I. Kaul, et al., Efficacy and safety of xanomeline-trospium chloride in schizophrenia: a randomized clinical trial, JAMA Psychiat. 81 (8) (2024) 749–756.
[6] W.P. Horan, et al., The impact of xanomeline and trospium chloride on cognitive impairment in acute schizophrenia: replication in pooled data from two phase 3 trials, Am. J. Psychiatry 182 (3) (2025) 297–306.
[7] J.T. Coyle, NMDA receptor and schizophrenia: a brief history, Schizophr. Bull. 38 (5) (2012) 920–926.
[8] D.T. Balu, The NMDA receptor and schizophrenia: from pathophysiology to treatment, Adv. Pharmacol. 76 (2016) 351–382.
[9] J.C. Neill, et al., Animal models of cognitive dysfunction and negative symptoms of schizophrenia: focus on NMDA receptor antagonism, Pharmacol. Ther. 128 (3) (2010) 419–432.
[10] G. Lee, Y. Zhou, NMDAR hypofunction animal models of schizophrenia, Front. Mol. Neurosci. 12 (2019) 185.
[11] G. Mercuriali, et al., The clock is ticking on schizophrenia: a study protocol for a translational study integrating phenotypic, genomic, microbiome and biomolecular data to overcome disability, Front. Psych. 15 (2024) 1451678.
[12] J.M. Monti, et al., Sleep and circadian rhythm dysregulation in schizophrenia, Prog. Neuropsychopharmacol. Biol. Psychiatry 43 (2013) 209–216.
[13] K. Wulff, et al., Sleep and circadian rhythm disruption in schizophrenia, Br. J. Psychiatry 200 (4) (2012) 308–316.
[14] W.H. Walker 2nd, et al., Circadian rhythm disruption and mental health, Transl. Psychiatry 10 (1) (2020) 28.
[15] S. Comai, G. Gobbi, Melatonin, melatonin receptors and sleep: moving beyond traditional views, J. Pineal Res. 76 (7) (2024) e13011.
[16] C. Cajochen, K. Kräuchi, A. Wirz-Justice, Role of melatonin in the regulation of human circadian rhythms and sleep, J. Neuroendocrinol. 15 (4) (2003) 432–437.
[17] C. Sahbaz, et al., Evidence for an association of serum melatonin concentrations with recognition and circadian preferences in patients with schizophrenia, Metab. Brain Dis. 34 (3) (2019) 865–874.
[18] M.L. Rao, et al., Circadian rhythm of tryptophan, serotonin, melatonin, and pituitary hormones in schizophrenia, Biol. Psychiatry 35 (3) (1994) 151–163.
[19] H.H. Okamoto, et al., Melatonin receptor structure and signaling, J. Pineal Res. 76 (3) (2024) e12952.
[20] G. Gobbi, S. Comai, Differential function of melatonin MT(1) and MT(2) receptors in REM and NREM sleep, Front. Endocrinol. (Lausanne) 10 (2019) 87.
[21] M. López-Canul, et al., Selective enhancement of REM sleep in male rats through activation of melatonin MT(1) receptors located in the locus ceruleus norepinephrine neurons, J. Neurosci. 44 (29) (2024).
[22] M. López-Canul, et al., Melatonin MT(1) and MT(2) receptors exhibit distinct effects in the modulation of body temperature across the light/dark cycle, Int. J. Mol. Sci. 20 (10) (2019).
[23] R. Ochoa-Sanchez, et al., Melatonin, selective and non-selective MT1/MT2 receptors agonists: differential effects on the 24-h vigilance states, Neurosci. Lett. 561 (2014) 156–161.
[24] M. Tassan Mazzocco, et al., Melatonin MT(1) receptors as a target for the psychopharmacology of bipolar disorder: a translational study, Pharmacol. Res. 198 (2023) 106993.
[25] Q.K. Lv, et al., Melatonin MT1 receptors regulate the Sirt1/Nrf2/Ho-1/Gpx4 pathway to prevent α-synuclein-induced ferroptosis in Parkinson's disease, J. Pineal Res. 76 (2) (2024) e12948.
[26] S.S. Andrabi, et al., Reversal of Schizophrenia-like symptoms and cholinergic alterations by melatonin, Arch. Med. Res. 50 (5) (2019) 295–303.
[27] Q. Wang, et al., Melatonin recovers sleep phase delayed by MK-801 through the melatonin MT(2) receptor- Ca(2+) -CaMKII-CREB pathway in the ventrolateral preoptic nucleus, J. Pineal Res. 69 (3) (2020) e12674.
[28] R. Saravani, et al., Melatonin receptor 1B gene polymorphisms, haplotypes and susceptibility to schizophrenia, Revista Romana De Medicina De Laborator 25 (2) (2017) 125–133.

[29] S. Rivara, et al., N-(Anilinoethyl)amides: design and synthesis of metabolically stable, selective melatonin receptor ligands, ChemMedChem 4 (10) (2009) 1746–1755.
[30] M. Lopez-Canul, et al., Selective melatonin MT2 receptor ligands relieve neuropathic pain through modulation of brainstem descending antinociceptive pathways, Pain 156 (2) (2015) 305–317.
[31] J. Wu, et al., Bimodal effects of MK-801 on locomotion and stereotypy in C57BL/6 mice, Psychopharmacology 177 (3) (2005) 256–263.
[32] R. Ochoa-Sanchez, et al., Anxiolytic effects of the melatonin MT(2) receptor partial agonist UCM765: comparison with melatonin and diazepam, Prog. Neuropsychopharmacol. Biol. Psychiatry 39 (2) (2012) 318–325.
[33] M. López-Canul, et al., Antinociceptive properties of selective MT(2) melatonin receptor partial agonists, Eur. J. Pharmacol. 764 (2015) 424–432.
[34] S. Nasini, et al., Age-Related Effects of Exogenous Melatonin on Anxiety-like Behavior in C57/B6J mice, Biomedicines 11 (2023) 1705.
[35] A. Inserra, et al., Effects of repeated lysergic acid diethylamide (LSD) on the mouse brain endocannabinoidome and gut microbiome, Br. J. Pharmacol. 180 (6) (2023) 721–739.
[36] R.M. Deacon, J.N. Rawlins, T-maze alternation in the rodent, Nat. Protoc. 1 (1) (2006) 7–12.
[37] S. Comai, D. De Gregorio, Hypnotic effects of melatonergic compounds measured in mice or rats, Methods Mol. Biol. 2550 (2022) 443–452.
[38] M.L. Dubocovich, et al., Selective MT2 melatonin receptor antagonists block melatonin-mediated phase advances of circadian rhythms, FASEB J. 12 (12) (1998) 1211–1220.
[39] A.A. Grace, Dysregulation of the dopamine system in the pathophysiology of schizophrenia and depression, Nat. Rev. Neurosci. 17 (8) (2016) 524–532.
[40] B. Lacoste, et al., Anatomical and cellular localization of melatonin MT1 and MT2 receptors in the adult rat brain, J. Pineal Res. 58 (4) (2015) 397–417.
[41] K. Cui, et al., Behavioral features and disorganization of oscillatory activity in C57BL/6J mice after acute low dose MK-801 administration, Front. Neurosci. 16 (2022) 1001869.
[42] M.R. Hudson, et al., NMDA receptors on parvalbumin-positive interneurons and pyramidal neurons both contribute to MK-801 induced gamma oscillatory disturbances: complex relationships with behaviour, Neurobiol. Dis. 134 (2020) 104625.
[43] M. Carlén, et al., A critical role for NMDA receptors in parvalbumin interneurons for gamma rhythm induction and behavior, Mol. Psychiatry 17 (5) (2012) 537–548.
[44] T. Hakami, et al., NMDA receptor hypofunction leads to generalized and persistent aberrant gamma oscillations independent of hyperlocomotion and the state of consciousness, PLoS One 4 (8) (2009) e6755.
[45] G. Buzsáki, X.J. Wang, Mechanisms of gamma oscillations, Annu. Rev. Neurosci. 35 (2012) 203–225.
[46] G. Gonzalez-Burgos, D.A. Lewis, NMDA receptor hypofunction, parvalbumin-positive neurons, and cortical gamma oscillations in schizophrenia, Schizophr. Bull. 38 (5) (2012) 950–957.
[47] P.J. Uhlhaas, W. Singer, Abnormal neural oscillations and synchrony in schizophrenia, Nat. Rev. Neurosci. 11 (2) (2010) 100–113.
[48] R. Ochoa-Sanchez, et al., Promotion of non-rapid eye movement sleep and activation of reticular thalamic neurons by a novel MT2 melatonin receptor ligand, J. Neurosci. 31 (50) (2011) 18439–18452.
[49] M. Notaras, et al., Schizophrenia is defined by cell-specific neuropathology and multiple neurodevelopmental mechanisms in patient-derived cerebral organoids, Mol. Psychiatry 27 (3) (2022) 1416–1434.
[50] F. Georgiadis, et al., Connectome architecture shapes large-scale cortical alterations in schizophrenia: a worldwide ENIGMA study, Mol. Psychiatry 29 (6) (2024) 1869–1881.
[51] R. Passiatore, et al., Changes in patterns of age-related network connectivity are associated with risk for schizophrenia, Proc. Natl. Acad. Sci. U. S. A. 120 (32) (2023) e2221533120.
[52] F. Fanget, et al., Nocturnal plasma melatonin levels in schizophrenic patients, Biol. Psychiatry 25 (4) (1989) 499–501.
[53] D. Viganò, et al., A study of light/dark rhythm of melatonin in relation to cortisol and prolactin secretion in schizophrenia, Neuro Endocrinol. Lett. 22 (2) (2001) 137–141.
[54] P. Monteleone, et al., Decreased nocturnal secretion of melatonin in drug-free schizophrenics: no change after subchronic treatment with antipsychotics, Neuropsychobiology 36 (4) (1997) 159–163.
[55] E.D. Mesa, et al., Seasonality of serum melatonin concentrations in paranoid schizophrenic inpatients, Eur. Neuropsychopharmacol. 20 (2010) S452.
[56] I. Antolín, et al., Neurohormone melatonin prevents cell damage: effect on gene expression for antioxidant enzymes, FASEB J. 10 (8) (1996) 882–890.
[57] R. Reiter, et al., The oxidant/antioxidant network: role of melatonin, Biol. Signals Recept. 8 (1–2) (1999) 56–63.
[58] S. Millán-Plano, et al., Melatonin and pinoline prevent aluminium-induced lipid peroxidation in rat synaptosomes, J. Trace Elem. Med Biol. 17 (1) (2003) 39–44.
[59] A. Dietrich-Muszalska, B. Olas, J. Rabe-Jablonska, Oxidative stress in blood platelets from schizophrenic patients, Platelets 16 (7) (2005) 386–391.
[60] J.K. Yao, S. Leonard, R. Reddy, Altered glutathione redox state in schizophrenia, Dis. Markers 22 (1–2) (2006) 83–93.
[61] E.I. Korotkova, et al., Study of OH radicals in human serum blood of healthy individuals and those with pathological schizophrenia, Int. J. Mol. Sci. 12 (1) (2011) 401–410.
[62] S. Comai, et al., Dysfunction of serotonergic activity and emotional responses across the light-dark cycle in mice lacking melatonin MT(2) receptors, J. Pineal Res. 69 (1) (2020) e12653.
[63] S. Comai, et al., Melancholic-like behaviors and circadian neurobiological abnormalities in melatonin MT1 receptor knockout mice, Int. J. Neuropsychopharmacol. 18 (3) (2015).
[64] X.Y. Yao, et al., Microglial Melatonin Receptor 1 Degrades Pathological Alpha-Synuclein through Activating LC3-Associated Phagocytosis In Vitro, CNS Neurosci. Ther. 30 (10) (2024) e70088.
[65] A. Aleman, R.S. Kahn, J.P. Selten, Sex differences in the risk of schizophrenia: evidence from meta-analysis, Arch. Gen. Psychiatry 60 (6) (2003) 565–571.
[66] C.M. Canuso, G. Pandina, Gender and schizophrenia, Psychopharmacol. Bull. 40 (4) (2007) 178–190.
[67] T.H. McGlashan, K.K. Bardenstein, Gender differences in affective, schizoaffective, and schizophrenic disorders, Schizophr. Bull. 16 (2) (1990) 319–329.
[68] K.K. Bardenstein, T.H. McGlashan, Gender differences in affective, schizoaffective, and schizophrenic disorders, A Review. Schizophr Res 3 (3) (1990) 159–172.
[69] J.F. Duffy, et al., Sex difference in the near-24-hour intrinsic period of the human circadian timing system, Proc. Natl. Acad. Sci. U. S. A. 108 (Suppl 3) (2011) 15602–15608.
[70] S.W. Cain, et al., Sex differences in phase angle of entrainment and melatonin amplitude in humans, J. Biol. Rhythms 25 (4) (2010) 288–296.
[71] G.K. Paschos, R. Lordan, G.A. FitzGerald, Intersection of sex and circadian biology, Curr. Opin. Physiol. 45 (2025) 100834.
[72] L.A. Brotto, A.M. Barr, B.B. Gorzalka, Sex differences in forced-swim and open-field test behaviours after chronic administration of melatonin, Eur. J. Pharmacol. 402 (1–2) (2000) 87–93.
[73] G.E. Bentley, N. Perfito, R.M. Calisi, Season- and context-dependent sex differences in melatonin receptor activity in a forebrain song control nucleus, Horm. Behav. 63 (5) (2013) 829–835.
[74] F. Ferrarelli, Sleep Abnormalities in Schizophrenia: State of the Art and next steps, Am. J. Psychiatry 178 (10) (2021) 903–913.
[75] D. Pritchett, et al., Evaluating the links between schizophrenia and sleep and circadian rhythm disruption, J. Neural Transm. (Vienna) 119 (10) (2012) 1061–1075.
[76] J.K. Russell, et al., M(1)/M(4)-preferring muscarinic cholinergic receptor agonist xanomeline reverses wake and arousal deficits in nonpathologically aged mice, ACS Chem. Neurosci. 14 (3) (2023) 435–457.